https://doi.org/10.1007/s41230-026-4186-6

Analysis and prediction of liquid metal film thickness in centrifugal spray forming process

Peng Li[1, 2, 3], *Shi-zhong Wei[2], **Xian-qing Lei[3], Lu Yang[2, 4], Bo Sun[2, 3], and Shuai-wu Tong[2, 4]

1. School of Intelligent Vehicle Engineering, Luoyang Institute of Science and Technology, Luoyang 471003, Henan, China

2. Joint Engineering Research Center for Abrasion Control and Molding of Metal Materials, Henan University of Science and Technology, Luoyang 471003, Henan, China

3. School of Mechatronics Engineering, Henan University of Science and Technology, Luoyang 471003, Henan, China

4. School of Materials Science and Engineering, Henan University of Science and Technology, Luoyang 471003, Henan, China

Copyright © 2026 Foundry Journal Agency

Abstract: To study how the key parameters in the centrifugal spray forming process affect the thickness of a liquid film, a two-dimensional numerical model was constructed in Fluent to dynamically track the interface between the liquid film and air. The effects of forming process conditions and physical properties of molten metal materials on the thickness distribution of liquid film were studied. The thickness of the liquid film generally decreases with the increase of radial distance. However, when a hydraulic jump occurs, the thickness of the liquid film increases sharply. Under a given flow rate, the occurrence of a hydraulic jump depends on the inlet diameter. The inlet diameter has a great influence on the liquid film thickness in the central area of the centrifugal disc but not in the edge area. The influences of the rotational speed and flow rate on the thickness of the liquid film are opposite. An increase in rotational speed leads to thinning of the liquid film at the edge, whereas an increase in flow rate increases the thickness of the liquid film at the same location. The influence of the temperature on the thickness of the liquid film is relatively small, indicating that temperature is not a decisive factor in this process. Through analysis, a model for predicting the thickness of the liquid film at the edge of the centrifugal disc was established on the basis of parameters such as the Weber number (*We*) and Onezog number (*Oh*). The numerical simulation results show that this prediction model can provide more accurate prediction results.

Keywords: centrifugal disc; liquid film thickness; prediction; gas-liquid two-phase flow; centrifugal spray forming

CLC numbers: TP391.9 **Document code:** A **Article ID:** 1672-6421(2026)06-807-08

1 Introduction

Ring parts play a key role in the field of major equipment because of their wide applications in wind power equipment (e.g., bearings and gears), aerospace (e.g., transition rings for launch vehicles), energy facilities (e.g., sealing rings for pressure vessels), and even nuclear energy (e.g., support structures for nuclear reactors)[1-7]. In recent years, with the increasing demand for lightweight aluminum alloy ring parts with high specific strength, excellent fracture toughness and corrosion resistance, greater requirements have been put forward for their manufacturing performance. Therefore, it is particularly important to study the manufacturing process of aluminum alloy ring parts. The traditional ring billet production method often involves multiple steps, such as high-temperature melting, casting, and billet opening, which not only consumes much energy but also has low production efficiency and is accompanied by material waste[8, 9]. This process is not ideal for the promotion of environmental protection and intelligent production. To address these problems, this study explores a centrifugal spray forming process with near-net forming characteristics[10, 11]. This process can directly

*Shi-zhong Wei

Male, born in 1966, a second-level professor. His research primarily focuses on wear-resistant metal materials, advanced refractory alloys, and extreme manufacturing processes. He has been honored with numerous prestigious awards, including 2 Second Prizes of the National Science and Technology Progress Award, 6 First Prizes at the provincial and ministerial levels, the Science and Technology Innovation Award of the Ho Leung Ho Lee Foundation, the National Innovation Award, and the Henan Provincial Science and Technology Outstanding Contribution Award.

E-mail: hnwsz@126.com

**Xian-qing Lei

E-mail: ly-lxq@163.com

Received: 2024-09-06; Revised: 2024-12-01; Accepted: 2024-12-05

form the required ring parts from metal powder or preform through high-speed rotation and spray molten metal in fewer processing links, which significantly improves production efficiency, reduces energy consumption and waste.

The principle of centrifugal spray forming is shown in Fig. 1. The basic process is as follows: the molten metal enters the high-speed rotating centrifugal disc through the duct, and the molten metal forms a thin liquid film under the action of the centrifugal force and flows along the disc surface[11]. When the liquid film on the surface of the centrifugal disc spreads to the edge, due to the difference in density between the metal melt and the air, the Rayleigh Taylor instability phenomenon occurs. This instability phenomenon promotes the generation of finger-like protrusions structures at the edge of the centrifugal disk. The finger-like protrusions structure is broken into droplets under the combined action of centrifugal force and surface tension. This progression is termed film formation, breakage, and fracture. To understand the flow characteristics of a liquid film on the surface of a centrifugal disc, researchers have adopted different methods to model it. For example, Li et al.[10] recently established a theoretical model of the steady-state flow of a liquid film on the surface of a centrifugal disc by using the D'Alembert principle and Newton's law of viscosity, and obtained the relationship between the thickness of the liquid film at the edge and the operating parameters. Zhao et al.[12, 13] also obtained similar conclusions by simplifying the Navier-Stokes equations, focusing on the characteristics of the liquid film on the wall of the rotor. Emslie et al.[14] adopted a simplified method and established a theoretical calculation framework for the distribution of liquid film thickness on the surface of a rotating disc under the assumptions that the radius of the disc is very large, the thickness of the liquid film is uniform in the radial direction, and the shear effect of the liquid-air interface is ignored.

The further work from Burns and his team[15] is an important supplement to this field. They used the resistance method, which is an experimental technique, to measure the average radial velocity of thin film flow. On this basis, the viscosity factor model was modified, making it more consistent with the experimental observation data. Pan et al.[16] explored the influence of liquid properties, operating conditions, and the size of the centrifugal disc on the thickness of the edge liquid film through numerical simulation. This is a key step in understanding the performance of the hydrodynamic system and helps to optimize the parameter selection in the design process. Wang's research[17] was more detailed and used three-dimensional granulation numerical simulation technology, focusing on the analysis of the microscopic mechanism of droplet formation, which revealed the dynamic process of microscale phenomena in complex flow fields, which was highly important for improving the understanding and control of droplet dispersion.

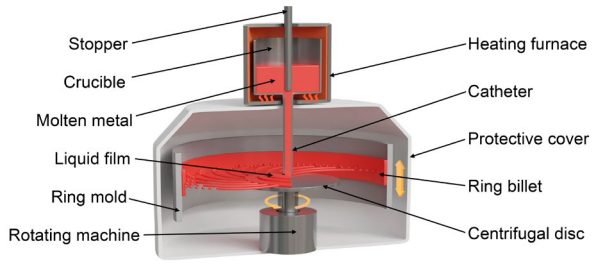


Fig. 1: Principle of centrifugal spray forming

To date, research on liquid film flow on the surface of a centrifugal disc has mainly focused on the flow state of the liquid film after it is thrown away from the edge of the disc and the size distribution of the droplets generated by its breakup. However, there are no systematic studies on the thickness of the liquid film on the surface of the centrifugal disc during the flow process. The lack of current research has made it difficult to establish a comprehensive relationship model, such as how the liquid film thickness is affected by the structure of the centrifugal disc, working conditions, and liquid metal characteristics. The insufficient research on liquid film thickness not only hinders in-depth exploration of the evolution mechanisms of metal droplets generated by liquid film breakup, but also imposes significant constraints on the precise optimization of process parameters in the centrifugal spray forming process.

This study is based on the principle of multiphase fluid dynamics and uses the VOF (volume of fluid)[18-20] method to simulate the real-time change in the liquid film and air interface on the surface of the centrifugal disc. A numerical model for the analysis of gas-liquid two-phase flow was established in the commercial software Fluent. This work not only lays a foundation for understanding and predicting the dynamic process of the transition from the edge liquid film to the droplet but also is highly important for the analysis of the droplet size distribution and heat transfer thermal analysis of the droplet during flight. The final goal is to provide a scientific basis for optimizing the experimental parameters of the centrifugal spray forming process.

2 Numerical model

2.1 Control equation

When the metal melt flows on the centrifugal surface, it exchanges heat with the external environment, resulting in changes in the physical parameters during flow. However, Pan et al.[18] reported that, through numerical simulation, owing to the very short time scale of the flow process, the change in the melt temperature can be ignored. Therefore, when analyzing the flow of metal melt on the surface of a centrifugal disc, it is usually assumed that the temperature of the metal melt does not change.

Under the complex action of air and a high-speed rotating disc, the metal liquid film on the centrifugal surface forms a typical gas-liquid two-phase stratified flow state with a free surface with air during the spreading flow process. In this work, the VOF[19-21] method was used to track the interface between the liquid film and air. The interface characteristics are obtained by solving the volume fraction continuity equation

and the equivalent momentum equation for the liquid film and air phases. In the calculation process, it is assumed that both the liquid film and air are incompressible Newtonian fluids[22-24] and that there is no mass or momentum transfer between the two phases. The continuity equation of the liquid film volume fraction can be expressed as:

$$\frac{\partial}{\partial t}\alpha_{\mathrm{L}}+\nabla\cdot\left(\alpha_{\mathrm{L}}\vec{u}_{\mathrm{L}}\right)=0 \tag{1}$$

where α_{L} is the volume fraction of the liquid film, and $\vec{u}_{\mathrm{L}}$ is the velocity vector of the liquid film.

The equivalent momentum equation of the liquid film and air is:

$$\frac{\partial\left(\rho\vec{u}\right)}{\partial t}+\nabla\cdot\left(\rho\vec{u}\times\vec{u}\right)=-\nabla P+\nabla\cdot\left[\mu\left(\nabla\vec{u}+\nabla\vec{u}^{T}\right)\right]+\rho g+\vec{F} \tag{2}$$

where $\vec{u}$ is the velocity vector of the mixed phase, P is the pressure, g is the acceleration of gravity, ρ and μ are the equivalent density and dynamic viscosity of the liquid film and air, respectively, and $\vec{F}$ is the momentum source term generated by the surface tension of the liquid film.

The equation for calculating the equivalent density and dynamic viscosity of the liquid film and air is as follows:

$$\rho=\alpha_{\mathrm{L}}\rho_{\mathrm{L}}+\left(1-\alpha_{\mathrm{L}}\right)\rho_{\mathrm{G}} \tag{3}$$

$$\mu=\alpha_{\mathrm{L}}\mu_{\mathrm{L}}+\left(1-\alpha_{\mathrm{L}}\right)\mu_{\mathrm{G}} \tag{4}$$

where ρ_{L} and ρ_{G} are the densities of the liquid film and air, respectively, and μ_{L} and μ_{G} are the dynamic viscosities of the liquid film and air, respectively.

According to the continuous surface tension model[25-27], the momentum source term $\vec{F}$ generated by the surface tension of the liquid film is calculated as:

$$\vec{F}=2\sigma\left(\nabla\cdot\frac{\vec{n}}{|\vec{n}|}\right)\frac{\rho\nabla\alpha_{\mathrm{L}}}{\rho_{\mathrm{L}}+\rho_{\mathrm{G}}} \tag{5}$$

where σ is the surface tension coefficient of the liquid film and $\vec{n}$ is the surface normal direction of the interface between the liquid film and air. The volume fraction α_{L} of the liquid film in each grid cell can be obtained by solving the volume fraction continuity Eq. (1) and the equivalent momentum Eq. (2) in the fluid calculation domain of the centrifugal disc. α_{L}=1 represents the liquid film in the grid cell, α_{L}=0 represents the air in the grid cell, and $0<\alpha_{\mathrm{L}}<1$ represents the coexistence of the liquid film and air in the grid cell. The interface position of the liquid film and air can be determined by the value of α_{L}=1.

2.2 Models and parameters

In the centrifugal spray forming process, the computational efficiency is improved by simplifying the complex three-dimensional process to a two-dimensional model. Further introduction of reasonable simplification assumptions (such as ignoring circumferential inhomogeneity and simplifying the boundary conditions of liquid film flow) to the two-dimensional model can further reduce the number of iterations and shorten the simulation period. Simplified centrifugal spray forming is shown in Fig. 2.

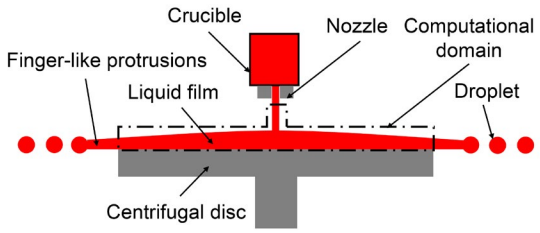


Fig. 2: Simplified centrifugal spray forming

The simplified rotational symmetry model, calculation domain and boundary are shown in Fig. 3. Its coordinate origin O is located at the center of the surface of the disc, the z-axis coincides with the centerline of the disc and points in the outer normal direction, and r is the radial direction of the disc. In Fig. 3, AO is the fixed axis of rotation with a height of H=6 mm and AB is the velocity inlet representing the liquid metal inlet flow. OE is the rotating wall with a radius of R=30 mm, while BC, CD, and DE are the pressure outlets.

In the numerical calculation, the relevant parameter settings in the model are shown in Table 1.

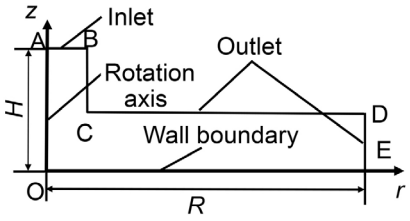


Fig. 3: Computational domain and boundary conditions

Table 1: Model parameters

Inlet diameter, d (mm)	Mass flow, Q_m (kg·min^{-1})	Rotational speed, N (r·min^{-1})
1, 2, 3, 5	2, 4, 6, 10	3,000; 4,000; 5,000; 7,000

Aluminum is widely used in the construction, aviation, automotive, packaging, and electronics industries[28-30]. It can be recycled and reused as an ideal material for a circular economy. Moreover, owing to the long history of industrial production of aluminum, a large number of experimental data and technical accumulations provide abundant resources for the determination of aluminum performance parameters. Therefore, this study took pure aluminum as the research object. The melting point of pure aluminum is 933 K, and the boiling point is 2,767 K[31, 32]. In the temperature range of 1,000–1,800 K, the changes in the physical properties of the droplet with temperature are shown in Table 2[31, 32].

2.3 Grid independence

Mesh independence means that the numerical solution is not sensitive to the change in mesh size, whereas model accuracy refers to whether the solution can accurately reflect the physical process. To verify the numerical model, three different meshes, Mesh 1 (0.03 mm in size, number 50,000), Mesh 2 (0.015 mm in size, number 180,000), and Mesh 3

Table 2: Variation in physical parameters of aluminum melt with temperature

Temperature T (K)	Density ρ (kg·m^{-3})	Surface tension σ (N·m^{-1})	Viscosity μ (mPa·s)
1,000	2,357	0.878	1.178
1,200	2,294	0.841	0.865
1,400	2,232	0.805	0.694
1,800	2,108	0.732	0.518

(0.01 mm in size, number 390,000), were used to calculate the liquid film thickness of the centrifugal disc. The set conditions included a mass flow rate of 3 kg·min^{-1}, a temperature of 1,000 K, and a rotational speed of 5,000 rpm. Figure 4 shows the verification of grid independence. Figure 4(a) shows the line chart of the liquid film thickness under different grids, and Fig. 4(b) shows the cloud map of the liquid film thickness. It can be seen from Fig. 4(a) that in the range of 25 mm to 30 mm at the edge of the centrifugal disc, the average thickness of the liquid film corresponding to Mesh 1, Mesh 2, and Mesh 3 is 0.041 mm, 0.045 mm, and 0.047 mm, respectively. The relative

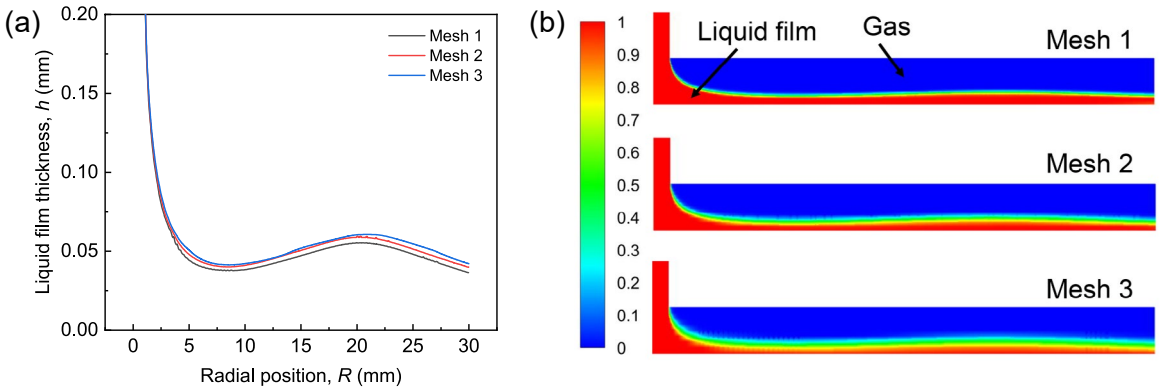


Fig. 4: Grid independence verification: (a) line chart; (b) cloud chart

error between Mesh 1 and Mesh 2 is 9.8 %, while the relative error between Mesh 2 and Mesh 3 is only 4.5%. It can be seen that when the mesh is refined, the difference of calculation results is gradually smaller, and the numerical accuracy tends to be consistent. Considering the calculation accuracy and calculation cost, Mesh 2 is selected for subsequent numerical calculation.

2.4 Model accuracy

Limited research has been conducted on the flow of liquid metal films over the surface of centrifugal discs. This study employs to the theoretical formula of liquid film thickness under the steady-state conditions in Ref. [10] to verify the numerical model. The theoretical value of the liquid film thickness can be calculated via Eq. (6):

$$h = \left(\frac{3\mu Q_V}{2\pi\rho R^2 \omega^2} \right)^{\frac{1}{3}} \quad (6)$$

where h is the liquid film thickness, ω is the speed of the centrifugal disc, R is the radius of the centrifugal disc, and Q_V is the volume flow rate.

Figure 5 shows the accuracy verification of the model. The liquid film thickness predicted via numerical simulation clearly shows hydraulic jump characteristics in its radial position; that is, the thickness changes suddenly. This is because the numerical model is obtained under transient conditions, and the liquid film at the hydraulic jump radius is in a strongly turbulent state. It is difficult for the theoretical model to calculate the thickness of the liquid film here. Nevertheless,

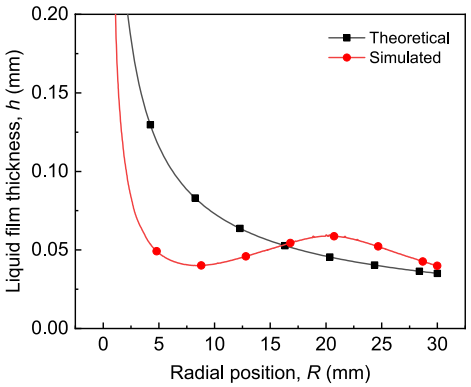


Fig. 5: Verification of model accuracy

the numerical simulation and theoretical calculation results are still consistent in terms of the general trend of the liquid film thickness and the edge value, which indicates that the numerical analysis method has good accuracy and credibility in dealing with such nonlinear problems.

3 Results and discussion

3.1 Effect of inlet diameter

At a temperature of 1,200 K, a flow rate of 6 kg·min^{-1}, and a rotational speed of 5,000 r·min^{-1}, the effects of different inlet diameters on the thickness distribution of the liquid film on the surface of the centrifugal disc are shown in Fig. 6. The data in Fig. 6 show that the inlet diameter exerts an influence on the liquid film thickness primarily in the central region of the centrifugal disc. The larger the inlet diameter, the thicker

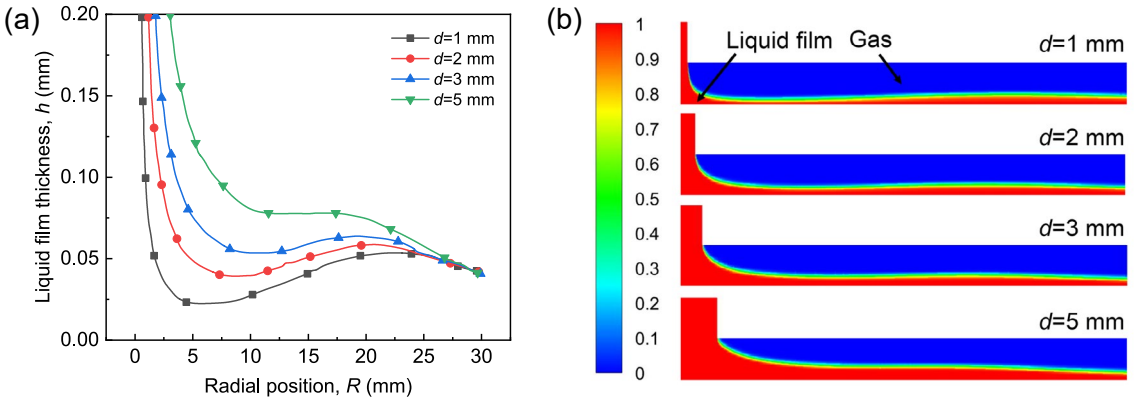


Fig. 6: Effect of different inlet diameters on thickness distribution of liquid film on centrifugal disc surface: (a) line chart; (b) cloud chart

the liquid column flowing to the surface of the centrifugal disc, and broader the influence range of the liquid column. Especially after the hydraulic jump, the sensitivity of the liquid film thickness to the inlet diameter is reduced. However, at the edge of the rotating disc, the liquid film thickness does not change much and remains relatively uniform regardless of the diameter, because the liquid flow pattern approaches a uniform distribution. Notably, when the inlet diameter is 5 mm, no hydraulic jump is observed on the surface of the centrifugal disc. This shows that the inlet diameter has a direct effect on the dynamic process governing hydraulic jump occur hence. In general, although the inlet diameter affects the characteristics of the liquid film in the central region, it has little effect on the liquid film distribution in the edge region.

3.2 Effect of flow

When the temperature is 1,200 K, the inlet diameter is 2 mm, and the rotational speed is 5,000 r·min^{-1}, the influence of different flow rates on the thickness distribution of the liquid film on the centrifugal disc surface is shown in Fig. 7. The diagram shows that the inlet flow rate has a significant effect on the thickness of the liquid film on the surface of the disc. With increasing flow rate, the liquid film thickness shows an overall increasing trend, and its variation exhibits obvious position dependence along the radial direction of the centrifugal disc. Under the constant circumferential dimension of the flow cross-section, a higher flow rate contributes to a thicker liquid film, and this effect becomes more significant with the increase of radial position. The diagram also shows that when the flow rate is less than 6 kg·min^{-1}, the liquid film thickness decreases sharply from the center to the edge of the centrifugal disc, then increases and finally decreases again gradually. When the flow rate is 10 kg·min^{-1}, the liquid film thickness drops sharply near the center and then rises continuously, reaching its maximum at approximately 25 mm from the center, with only a slight decrease at the outermost edge. When the liquid film thickness falls within the range of the hydraulic jump radius, its reduction with increasing flow rate is not pronounced. This is because a higher inlet pouring flow rate leads to a higher radial spreading velocity of the liquid film on the surface of the centrifugal disc, which further extends the region affected by the hydraulic jump and allows the liquid film to cover a larger area. Once the liquid film propagates to the boundary of the hydraulic jump radius, a local abrupt change occurs at this radial position, resulting in a marked increase in the liquid film thickness at the hydraulic jump radius. As the liquid film further flows outward along the radial direction, the increase in radial size not only increases the surface area of the liquid film but also increases the centrifugal force. The strong centrifugal force accelerates the flow velocity of the liquid film, and the combination of the two makes the liquid film thinner after the hydraulic jump.

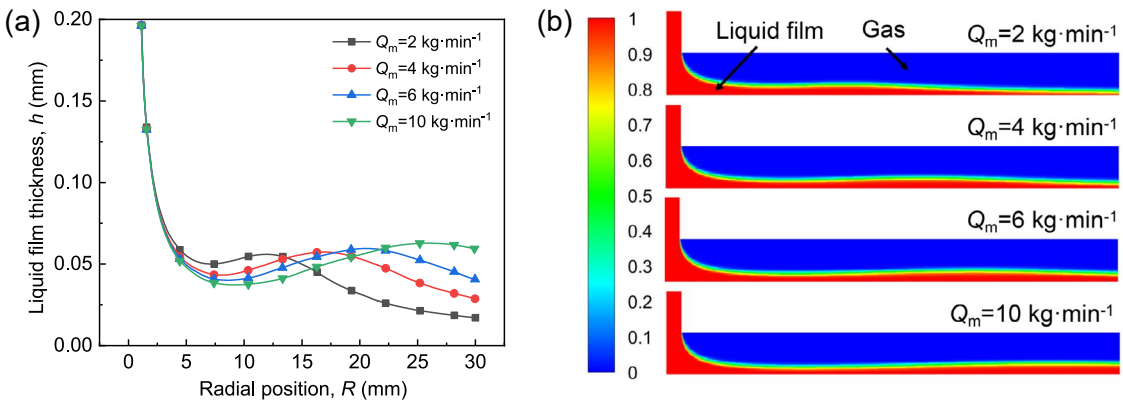


Fig. 7: Effects of different flow rates on thickness distribution of liquid film on centrifugal disc surface: (a) line chart; (b) cloud chart

3.3 Effect of rotational speed

When the temperature is 1,200 K, the inlet diameter is 2 mm, and the flow rate is 6 kg·min^{-1}, the influence of different rotational speeds on the thickness distribution of the liquid film on the surface of the centrifugal disc is shown in Fig. 8. The rotational speed has a significant effect on the thickness of the liquid film, showing a negative correlation. In the area near the center of the centrifugal disc, the liquid film thickness does not change much, because it is affected mainly by the liquid column flowing from the inlet to the rotary disc surface rather than rotational speed. However, as the liquid flow gradually moves away from the center, the effect of the rotational speed becomes more obvious, and the liquid film thickness decreases with increasing rotational speed. This is because the higher rotational speed enhances the shear force of the fluid relative to the centrifugal disc, accelerating its radial outward flow and consequently thinning the liquid film. However, when the rotational speed is further increased to a sufficiently high level, the reduction rate of liquid film thickness in the edge region gradually slows down and tends to stabilize. This occurs because the liquid film has already reached a relatively stable thin-layer state under strong centrifugal driving, with its flow governed by inertial forces rather than viscous effects, leaving little room for further thickness reduction. Accordingly, simply increasing the rotational speed can no longer realize the refined and effective regulation of liquid film thickness. Therefore, in practical operation, it is necessary to comprehensively consider the rotational speed and the other parameters to find the optimal working conditions to obtain the ideal liquid film thickness distribution.

3.4 Effect of pouring temperature

When the inlet diameter is 2 mm, the rotational speed is 5,000 r·min^{-1}, and the flow rate is 6 kg·min^{-1}, the influence of different pouring temperatures on the thickness distribution of the liquid film on the surface of the centrifugal disc is shown in Fig. 9. The diagram shows that the change in temperature has no significant effect on the liquid film thickness distribution at the edge but has a significant effect on the intermediate process. As the temperature decreases, the thickness of the liquid film at the middle position of the centrifugal disc increases significantly. This phenomenon can be attributed to two reasons. First, a decrease in temperature leads to an increase in liquid metal density, which raises the static pressure within the liquid film. The increased pressure intensifies the flow resistance and hinders the outward spreading of the molten liquid film. Second, as the temperature decreases, the viscosity of the liquid increases accordingly, which aggravates the frictional resistance inside the fluid and slows the radial fluidity, thus increasing the thickness of the liquid film. Although the overall effect of temperature on the film thickness is relatively small, it has a decisive influence on the heat transfer efficiency. At high temperatures, excessively fast heat transfer may lead to uneven crystallization, and the degree of crystal refinement depends on the heat transfer efficiency. Therefore, to obtain a uniform small grain structure and reduce

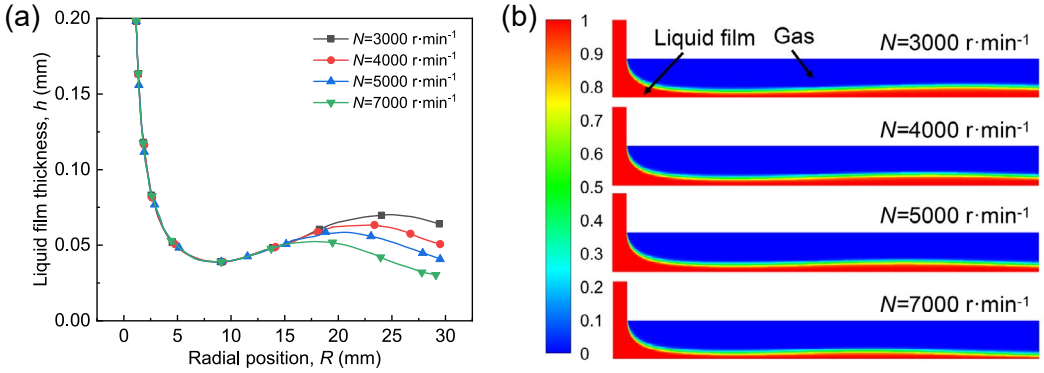


Fig. 8: Effect of different rotational speeds on thickness distribution of liquid film on centrifugal disc surface: (a) line chart; (b) cloud chart

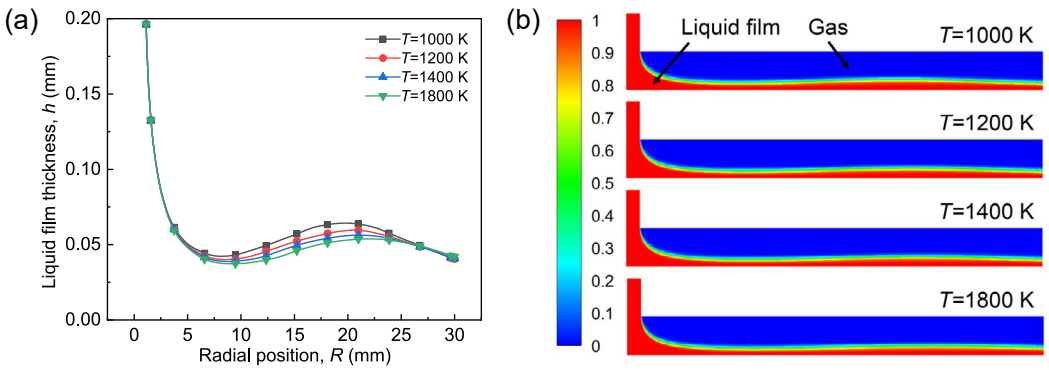


Fig. 9: Effects of different temperatures on thickness distribution of liquid film on centrifugal disc surface: (a) line chart; (b) cloud chart

energy consumption, it is necessary to accurately control the temperature of the molten metal while ensuring that the melt can form droplets and flow through the liquid film to achieve the best heat transfer and crystallization effects.

3.5 Liquid film thickness prediction

The thickness of the liquid film has an important influence on the diameter and distribution of the droplets generated by subsequent atomization process. However, in the centrifugal spray forming process, especially in the theoretical model, it is difficult to fully capture the liquid film behavior on the complex surface of the centrifugal disc. In this study, the dimensionless analysis method was used to simplify the problem. The liquid film thickness can be expressed by a comprehensive dimensionless expression, as shown in Eq. (7). The expression takes into account key factors such as the flow rate, physical properties, and rotational speed. This analysis helps researchers better design and optimize the centrifugal spray forming process and therefore obtain the desired particle size and shape distribution.

$$h = f\left(Q_{\mathrm{m}}, R, \rho, \mu, \sigma, \omega\right) \tag{7}$$

Through the dimensionless analysis of the Π theorem, the following can be obtained:

$$\frac{h}{R} = a\Pi_1^b \Pi_2^c \Pi_3^d \tag{8}$$

$$\Pi_1 = \frac{Q_{\mathrm{m}}}{\omega R^3} \tag{9}$$

$$\Pi_2 = Oh = \frac{\mu}{\sqrt{\rho R \sigma}} \tag{10}$$

$$\Pi_3 = We = \frac{\rho \omega^2 R^3}{\sigma} \tag{11}$$

where a, b, c, and d are undetermined constants, Oh is the Onyzog number, We is the Weber number, and Π_1, Π_2, and Π_3 are dimensionless parameters.

On the basis of the data obtained via numerical calculation, the coefficients a, b, c, and d can be obtained via multivariate nonlinear regression analysis, then Eq. (12) can be obtained. The applicable conditions of this equation are $\Pi_1 = 7.34\times10^{-4} - 5.14\times10^{-3}$, $\Pi_2 = 7.61\times10^{-5} - 4.50\times10^{-4}$, $\Pi_3 = 7.27\times10^{3} - 3.96\times10^{4}$.

$$\frac{h}{R} = 0.244\left(\frac{Q_{\mathrm{m}}}{\omega R^3}\right)^{2.421}\left(\frac{\mu}{\sqrt{\rho R\sigma}}\right)^{-3.720}\left(\frac{\rho\omega^2 R^3}{\sigma}\right)^{0.996} \tag{12}$$

Figure 10 shows the regression analysis diagram, showing that the equation can accurately predict the thickness of the liquid film at the edge of the centrifugal disc, which can provide a theoretical basis for the optimization of the subsequent centrifugal spray forming process.

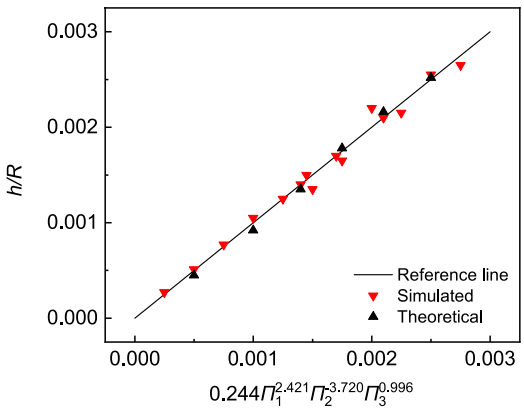


Fig. 10: Regression relationship between h/R and $0.244\Pi_1^{2.421}\Pi_2^{-3.720}\Pi_3^{0.996}$

4 Conclusions

(1) When the inlet flow rate and physical parameters are constant, the inlet diameter has almost no direct effect on the liquid film thickness in the edge region of the centrifugal disc. This means that the diameter distribution after the liquid film is broken into droplets is not related to the initial inlet diameter, which helps to understand the stability of the liquid film treatment process.

(2) The rotational speed has a negative correlation with the liquid film thickness in the edge of the centrifugal disc; that is, the higher the rotational speed, the thinner the liquid film. However, this trend is not infinite. As the rotational speed increases, the trend of decreasing liquid film thickness gradually weakens, which means that simply increasing the rotational speed cannot reduce the liquid film thickness unlimitedly. In contrast, the effect of the flow rate shows a possitive correlation with the liquid film thickness at the edge of the centrifugal disc; that is, the larger the flow rate, the thicker the liquid film.

(3) The effect of temperature on the liquid film thickness is not significant, which means that the temperature can be adjusted appropriately without significantly changing the liquid film characteristics when controlling the process flow.

(4) On the theoretical level, through the dimensional analysis method, researchers have found an equation describing the relationship between the liquid film thickness at the edge of the centrifugal disc and the flow rate (dimensionless), Weber number, and Onezog number, namely equation $\frac{h}{R} = 0.244\left(\frac{Q_{\mathrm{m}}}{\omega R^3}\right)^{2.421}\left(\frac{\mu}{\sqrt{\rho R\sigma}}\right)^{-3.720}\left(\frac{\rho\omega^2 R^3}{\sigma}\right)^{0.996}$. Through simulation verification, this equation is proven to be able to accurately predict the liquid film thickness distribution to guide the optimal design in practical operation.

Acknowledgment

This work was financially supported by the National Key R&D Program of China (2020YFB2008400).

Conflict of interest

The authors declare that they have no known competing financial interests or personal relationships that could have appeared to influence the work reported in this paper.

References

[1] Mao X C, Yi Y P, He H L, et al. Second phase particles and mechanical properties of 2219 aluminum alloys processed by an improved ring manufacturing process. Materials Science & Engineering: A, 2020, 781: 139226.
[2] Noraphaiphipaksa N, Poapongsakorn P, Hasap A, et al. Failure analysis of pressure vessel with sight ports using finite element analysis. Engineering Failure Analysis, 2020, 117: 104791.
[3] Pu Q Q, Jia Z H, Kong Y P, et al. Microstructure and mechanical properties of 2195 alloys prepared by traditional casting and spray forming. Materials Science & Engineering: A, 2020, 784: 139337.
[4] Hussain S, Cui C S, Temple N, et al. Porosity and microstructure of steel tubes spray-formed by close-coupled atomizer. Journal of Materials Processing Technology, 2019, 276: 116407.
[5] Tian D Y, Han X H, Hua L, et al. A novel process for axial closed extrusion of ring part with mesh-like ribs. International Journal of Mechanical Sciences, 2020, 165: 105186.
[6] Ni Y, Li Y G, Liu C Q, et al. A mechanism informed neural network for predicting machining deformation of annular parts. Advanced Engineering Informatics, 2022, 53: 101661.
[7] Zou H, Wang S, Chen P, et al. Global dynamic characteristics analysis of GTF star gear transmission system considering ring gear elastic deformation. Thin-Walled Structures, 2024, 198: 111712.
[8] Qin F C, Qi H P, Li Y T, et al. Advances in compact cast-rolling forming of ring-shape parts. Materials Reports, 2020, 34(19): 19152–19165.
[9] Qin F C, Qi H P, Li Y T, et al. Technology of integrated manufacturing in forming and modification of aluminum alloy rings. Materials Reports, 2021, 35(9): 9049–9058.
[10] Li P, Wei S Z, Lei X Q, et al. Modeling and analysis of metal liquid film flow characteristics during centrifugal spray forming. Metals, 2023, 13(10): 1687.
[11] Li P, Wei S Z, Lei X Q, et al. Study on flight dynamics and heat transfer solidification of metal droplets during centrifugal spray deposition forming process. Metals, 2023, 13(8): 1446.
[12] Zhao Y Y. Analysis of flow development in centrifugal atomization: Part I. Film thickness of a fully spreading melt. Modeling and Simulation in Materials Science and Engineering, 2004, 12(5): 959.
[13] Zhao Y Y. Analysis of flow development in centrifugal atomization: Part II. Disintegration of a nonfully spreading melt. Modeling and Simulation in Materials Science and Engineering, 2004, 12(5): 973.
[14] Emslie A G, Bonner F T, and Peck L G. Flow of a viscous liquid on a rotating disc. Journal of Applied Physics, 1958: 1723300.
[15] Burns J R, Ramshaw C, and Jachuck R J. Measurement of liquid film thickness and the determination of spin-up radius on a rotating disc using an electrical resistance technique. Chemical Engineering Science, 2003, 58(11): 2245–2253.
[16] Pan Y H, Witt P J, Kuan B, et al. CFD modeling of the effects of operating parameters on the spreading of liquids on a spinning disc. The Journal of Computational Multiphase Flows, 2014, 6(1): 49–64.
[17] Wang D, Ling X, and Peng H. Simulation of ligament mode breakup of molten slag by spinning disc in the dry granulation process. Applied Thermal Engineering, 2015, 84: 437–447.
[18] Pan Y H, Witt P J, and Xie D. CFD simulation of free surface flow and heat transfer of liquid slag on a spinning disc for a novel dry slag granulation process. Progress in Computational Fluid Dynamics, An International Journal, 2010, 10(5–6): 292–299.
[19] Mulbah C, Kang C, Mao N, et al. A review of VOF methods for simulating bubble dynamics. Progress in Nuclear Energy, 2022, 154: 104478.
[20] Sun J, Liu Q, Liang Y, et al. Three-dimensional VOF simulation of droplet impacting on a superhydrophobic surface. Bio-Design and Manufacturing, 2019, 2: 10–23.
[21] Wen H L, Yu C H, and Sheu T W H. On the development of LS-assisted VOF method for incompressible interfacial flows. Journal of Computational Physics, 2019, 406: 109188.
[22] Panahi A, Pishevar A R, and Tavakoli M R. Numerical simulation of jet mode in electrospraying of newtonian and viscoelastic fluids. International Journal of Multiphase Flow, 2020, 129: 103302.
[23] Rahman M M and Faghri A. Numerical simulation of fluid flow and heat transfer in a thin liquid film over a rotating disk. International Journal of Heat and Mass Transfer, 1992, 35(6): 1441–1453.
[24] Wang Q F, Li M X, Xu W J, et al. Review on liquid film flow and heat transfer characteristics outside horizontal tube falling film evaporator: Cfd numerical simulation. International Journal of Heat and Mass Transfer, 2020, 163: 120440.
[25] Duan R, Sun C, and Jiang S. A new surface tension formulation for particle methods. International Journal of Multiphase Flow, 2020, 124: 103187.
[26] Wu J, Yu S T, and Jiang B N. Simulation of two-fluid flows by the least-squares finite element method using a continuum surface tension model. International Journal for Numerical Methods in Engineering, 1998, 42(4): 583–600.
[27] Zhao C H, Maarek J, Taleghani S M, et al. A hybrid continuum surface tension force for the three-phase VOF method. Journal of Computational Physics, 2024, 504: 112872.
[28] Wu G H, Guo Y J, Qi F Z, et al. Role of alloying and heat treatment on microstructure and mechanical properties of cast Al-Li alloys: A review. China Foundry, 2024, 21(5): 445–460.
[29] Wang Q G, Wang A, and Coryell J. Ultra-large aluminum shape casting: Opportunities and challenges. China Foundry, 2024, 21(5): 397–408.
[30] Yang Y, Luo Z, Zhang Y, et al. Dissimilar welding of aluminium to steel: A review. Journal of Manufacturing Processes, 2024, 110: 376–397.
[31] Li F C, Hu C B, Fu Y, et al. Rebound characteristics of burning aluminum droplets impacting surfaces. Aerospace Science and Technology, 2023, 133: 108127.
[32] Li F C, Fu Y, Li C, et al. Flowing characteristics of aluminum droplets impacting curved surface. Acta Physica Sinica, 2022, 71(18): 181–193.